Multi-ion conduction bands in a simple model of calcium ion channels

I. Kaufman[1], D.G. Luchinsky[1,2], R. Tindjong[1], P.V.E. McClintock[1*] and R.S. Eisenberg[3]

[1] Department of Physics, Lancaster University, Lancaster, LA1 4YB, UK;
[2] NASA Ames Research Center, MS 269-3, Moffett Field, CA, 94035, USA;
[3] The Department of Molecular Biophysics and Physiology, Rush Medical College, IL 60612, USA

Abstract
We report self-consistent Brownian dynamics simulations of a simple electrostatic model of the selectivity filters (SF) of calcium ion channels. They reveal regular structure in the conductance and selectivity as functions of the fixed negative charge Q_f at the SF. This structure comprises distinct regions of high conductance (conduction bands) M0, M1, M2 separated by regions of zero-conductance (stop-bands). Two of these conduction bands, M1 and M2, are related to the saturated calcium occupancies of P=1 and P=2, respectively and demonstrate self-sustained conductivity. Despite the model's limitations, its M1 and M2 bands show high calcium selectivity and prominent anomalous mole fraction effects and can be identified with the L-type and RyR calcium channels.

E-mail: p.v.e.mcclintock@lancaster.ac.uk;

Introduction

Voltage-gated calcium ion channels play an important role in stimulating muscle contraction, in neurotransmitter secretion, gene regulation and transmission of action potentials, based on their high selectivity for divalent calcium ions Ca^{2+} over monovalent sodium ions Na^+. They exhibit the Anomalous Mole Fraction Effect (AMFE), an effective blockade of Na^+ permeation by small concentrations of Ca^{2+}, combined with measurable Ca^{2+} currents in the pA range (1).

The selectivity of calcium channels is defined by a narrow selectivity filter (SF) with a strong binding site formed by negatively-charged protein residues (1, 2). Wild-type calcium channels and their mutants differ in the composition, structure (locus) and net fixed charge Q_f of these protein residues at the SF. The most-studied L-type calcium channel possesses an EEEE locus with an estimated Q_f=3-4e (2, 3), where e=-1.6x10^{-19}C. The ligand-gated Ryanodine receptor (RyR) calcium channel has a DDDD locus with a larger $Q_f{\approx}4.5e$ (4). The L-type and RyR channels exhibit different threshold concentrations for blockage of Na^+ current by Ca^{2+} ions: $[Ca]_{50}{\approx}1\mu M$ and $[Ca]_{50}{\approx}1mM$ respectively (4).

Mutant studies show that Q_f is crucial in determining the selectivity of the calcium channel. Usually, mutations that influence Q_f also destroy the channel's selectivity and hence physiological functionality (5). However, an appropriate point mutation of the DEKA sodium channel ($Q_f \approx 1e$) converts it into a calcium-selective channel with a DEEA locus and $Q_f \approx 4e$ (6). The essentially nonselective bacterial OmpF porin ($Q_f \approx 1e$) can be also turned into a Ca-selective channel by introduction of two additional glutamates in the constriction zone. The resultant mutant contains a DEEE-locus ($Q_f \approx 4e$) and demonstrates a Na current with a strongly increased sensitivity to 1 mM Ca (7).

Dynamic Monte-Carlo simulations of the flexible volume exclusion model of calcium and sodium channels (3, 8) show that the charge density at the SF is the first-order determinant of selectivity (3); and the Na^+ to Ca^{2+} occupancy ratio decreases monotonically as Q_f increases from 1e (DEKA locus) to 4e (DEEE locus), while the pore becomes more and more Ca^{2+} selective (9).

Self-consistent Brownian dynamics (BD) simulations (2) of conductance and selectivity, based on a purely electrostatic model of the L-type channel with a rigid binding site, revealed a narrow peak in Ca^{2+} conductance near Q_f=3.2e. (2, 10)

Although mutant studies (5-7) and simulations (2, 3, 9) have demonstrated very clearly the dominant influence of Q_f on the selectivity of the calcium channel, it has remained unclear why particular values of Q_f should be optimal for selectivity or how many such values may exist.

Multi-ion knock-on single-file conductivity (11-14) is assumed to be one of the possible mechanisms allowing to resolve the paradox of high selectivity and high conductance in calcium ion channel (15, 16), The discreteness of the ionic occupancy plays a significant role in channel conductivity and is expected to manifest as discrete multi-ion steps/bands in the dependences of occupancy and conductance on concentration, time and other parameters (17-19). These steps/bands are related to barrier-less knock-on conduction mechanism that has been suggested as being the underlying mechanism responsible for the conductivity and selectivity of ion channels (14)

In this article, we show that the Ca^{2+} conductance and selectivity of a simple model of calcium channels forms a regular structure of conduction/selectivity bands (regions) as a function of Q_f, separated by non-conduction bands, related to saturated, barrier-less, conductivity with different numbers of Ca^{2+} ions involved in the conduction. The conductance peak obtained in (2) is one part of this structure. We infer that all calcium-selective channels (both wild-type and mutants) should correspond to one of these bands.

Methods

The reduced axis-symmetrical model (Figure 1) represents the selectivity filter (SF) of a calcium ion channel (2, 3). Extracellular (left) and intracellular (right) baths are filled by ionic sodium-only, calcium-only or mixed sodium-calcium in-water solution. In this research we use an asymmetrical ionic concentration: $C_L>0$, $C_R=0$.
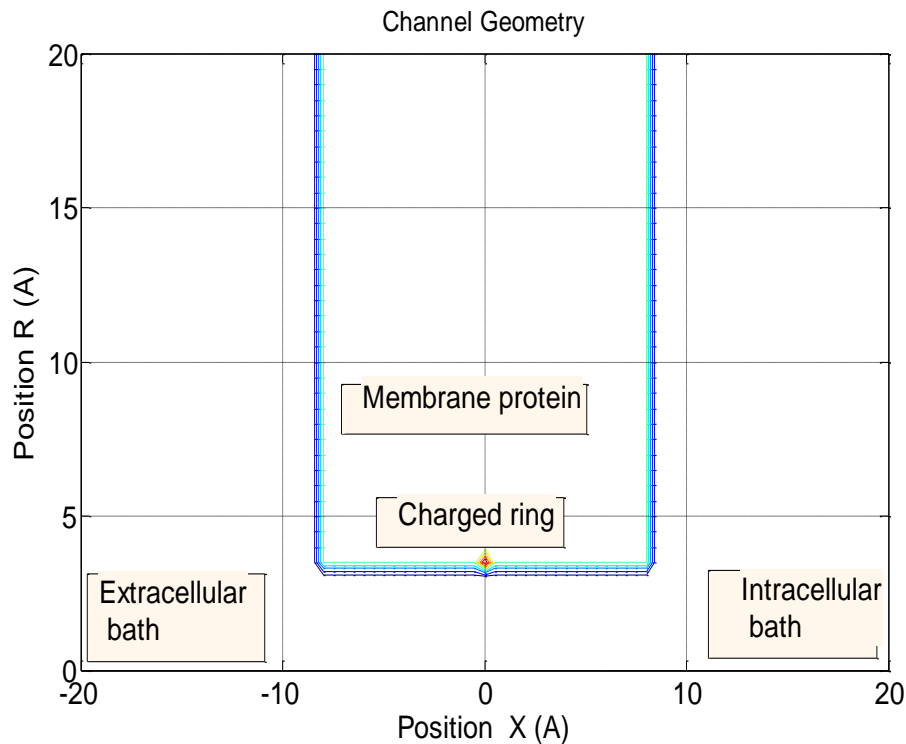

Figure 1. Reduced axis-symmetrical model of the calcium ion channel. The selectivity filter of a calcium ion channel is modelled as a water-filled cylindrical hole of radius R=3Å and length L=16Å through the protein hub in a cellular membrane with a centrally-placed uniformly-charged rigid ring with negative charge Q_f=0-6.5e. The right-hand bath (modeling extracellular space) contains a non-zero concentrations of Ca^{2+} and Na^+ ions.

The minimum possible radius R of the SF of an L-type calcium channel has been determined as being R=2.8Å. We use the value of R=3.0Å. We choose the length L=16Å as being close to the parameter value used in (3) . Moving sodium and calcium ions are described as charged particles of radius $R_i \approx 1$Å (matching both ions), with diffusion coefficients of D_{Na}=1.17x10^{-9} m^2/s and D_{Ca}=0.79 x 10^{-9} m^2/s, respectively.

Negatively-charged protein residues are modelled as forming a single, thin, uniformly-charged, centrally-placed, rigid ring around the SF. This ring is located inside the wall and brings a net negative charge Q_f of 0- 6.5e.

The electrostatic forces were derived self-consistently by numerical solution of Poisson's equation with respect to the ion-ion interaction, channel geometry (Figure 1), self-potential barrier of the dielectric boundary force (20), value of Q_f and value of applied potential V.

Our reduced model of the SF takes both water and protein to be homogenous continua with dielectric constants ε_w=80 and ε_p=2, respectively, together with a primitive model of ion hydration. The self-consistent electrostatics of a narrow, water-filled, channel in the protein wall results in the axial quasi-1D behaviour of the electrostatic field, and hence in single-file movement of positive ions inside the channel (21). Electrostatics also prohibits the entrance of any negatively charged ions (20). Thus we simulate cations-only movement inside the SF and in its close vicinity as axial single-file movement.

The BD simulations are based on numerical solution of the 1D over-damped Langevin equation:

$$x' = -Du_x + \sqrt{2D}\xi(t) \dots\dots\dots\dots\dots\dots\dots\dots\dots\dots\dots\dots\dots\dots\dots\dots\dots\dots\dots\dots\dots\dots(1)$$

where x stands for the ion's position, D is its diffusion coefficient, u is the self-consistent potential in $k_B T/e$ units, and $\xi(t)$ is normalized white noise.

We use an injection scheme where moving ions are injected randomly close to the left vicinity of the SF with an arrival rate that simulates the diffusive ionic flux from the undisturbed bulk with concentration C through the Smoluchowski diffusion rate J_{arr}=$2\pi DRC$. Simulations were performed with applied voltage V=0mV corresponded to depolarised membrane.

The validity of continuum electrostatics and Langevin dynamics for narrow channels is roughly defined by the relationship between the channel radius R and the radius of the ion's first hydration shell R_h (22); $R_h \approx 3.5$Å for Na$^+$ and Ca^{2+} ions. The calcium channel with $R\approx$ 3 Å (1) provides some room for Na$^+$ and Ca^{2+} ions to pass water molecules (22), so that the continuum approximation still can be used inside the SF but with *effective values* of ε_w and diffusion coefficients D_{Na}, D_{Ca} that are all dependent on R (22). It is shown in (22) that the effective ε_w saturates to its bulk value ε_w=80 for $R\approx3.5$ Å (roughly corresponding to R_h) and still close to it ($\varepsilon_w \approx 70$) for R=3Å. The effective ionic diffusion coefficients also decreased with decreasing R in comparison with bulk values (23).

In this investigation we use the bulk values of ε_w and D as their effective values throughout the whole compatational domain including the SF. This simplified model represents a considerable simplification of the actual electrostatics and dynamics of moving ions and water molecules in single-file within the narrow SF (23, 24).

The BD simulations of ion current J and occupancy P were performed separately for CaCl$_2$ and NaCl solutions, and also for a mixed-salt configuration, with concentrations *[Na]*=30mM and 20μM ≤ *[Ca]* ≤ 80mM. The value of Q_f was varied within the range 0-6.5e in order to cover the known variants of sodium and calcium channels (9).

Results and discussion

Fig. 1 (a) and (b) demonstrate our main result - the appearance of regular structure in the Ca^{2+} ion current J as a function of Q_f, and *[Ca]* comprising areas of high conductance (conduction bands) M0, M1, M2 separated by zero-conductance stop-bands. The peak separation $\Delta Q \approx 2e$ corresponds roughly to the charge on one Ca^{2+} ion. Band M1 coincides with the J peak from (2) .
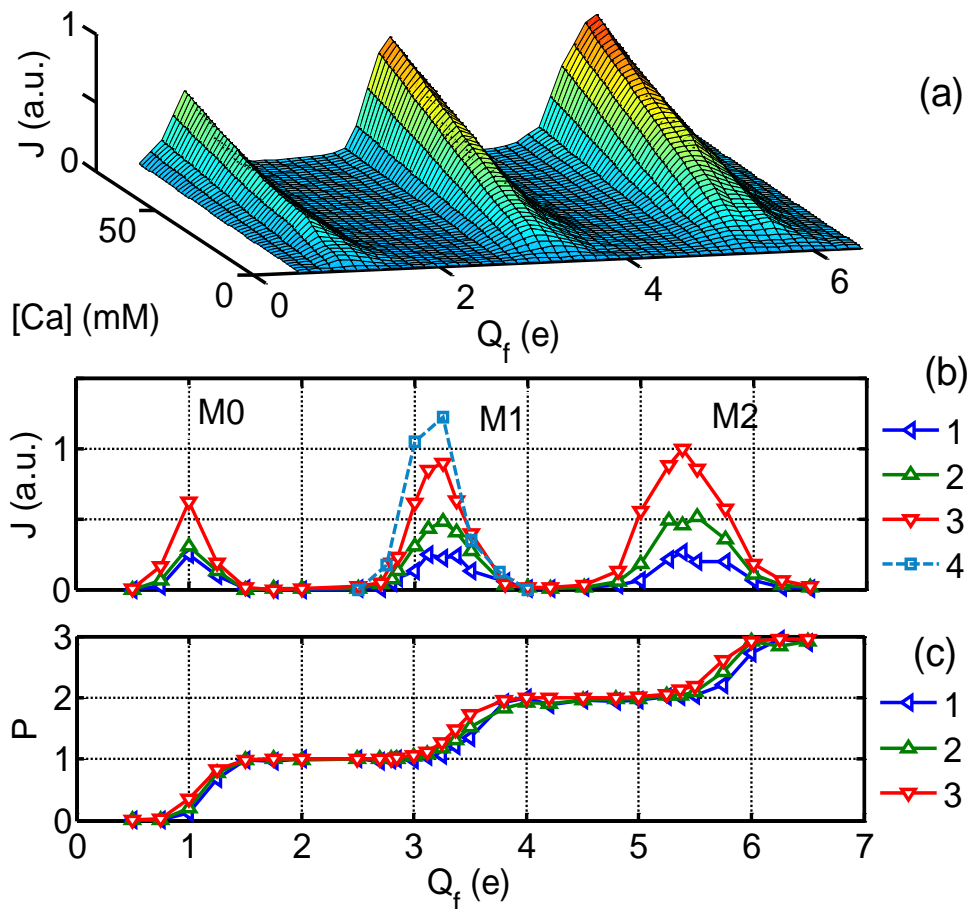

FIGURE 2. Multi-ion conduction bands of the calcium channel model.
(a) A 3D plot of the calcium current *J* vs fixed charge *Q_f* and concentration *[Ca]* exhibits regular band structure.
(b) A plot of *J* as a function of *Q_f* and *[Ca]* shows the M0, M1, and M2 bands: *plots 1,2,3 are J* and *P* for *[Ca]*=20mM, 40mM and 80mM, respectively; and 4 is the *J* peak from (2), corresponding to M1.
(c) The occupancy *P* shows stepwise growth as *Q_f* increases. The flat steps correspond to the saturated occupancy values *P*=1,2,3,..

The Ca^{2+} occupancy P exhibits step-wise growth with increasing Q_f (Fig. 1 (c)). The flat steps correspond to non-conducting saturated states with $P=0,1,2\ldots$ where the potential well at the binding site is too deep to allow escape of a Ca^{2+} ion and too shallow to allow the next Ca^{2+} ion to enter the SF and push the bound ion(s) out. The conduction bands M0, M1 and M2 correspond to transitions in P: $0\rightarrow1$, $1\rightarrow2$, and $2\rightarrow3$, respectively. This picture corresponds to the "knock-on" mechanism of Ca^{2+} conductance

4

and selectivity (1, 2). It has an obvious analogue in semiconductor physics, where conduction also occurs in partially filled bands (25).

The appearance of distinct conduction bands is caused by the discreteness of the multi-ion occupancy P. Their existence just for Ca^{2+} in the calcium channel relates to the high Q_f and double-valence of Ca^{2+}, enhancing the electrostatic effects of valence selectivity (10).
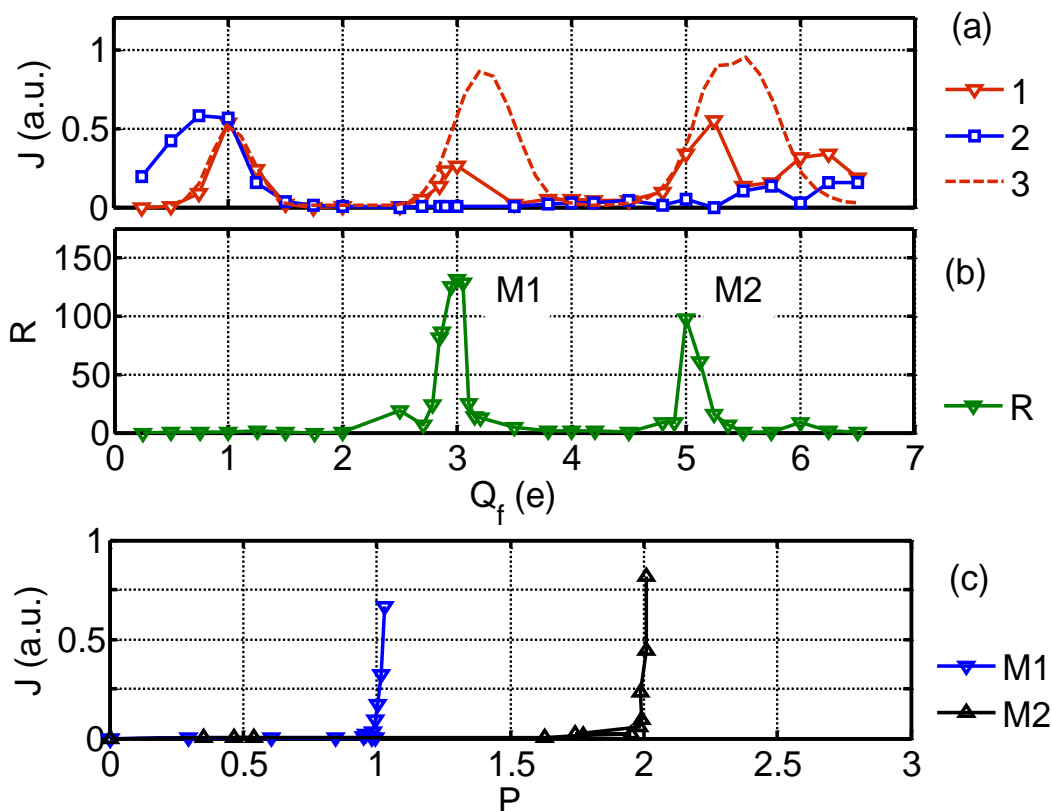

FIGURE 3. Conduction and selectivity bands for a *[Na]=30mM, [Ca]=40mM* mixed salt bath.
(a) Currents *J vs* fixed charge *Q_f*. Curves: 1 - Ca, 2 - Na, 3 – Ca for a pure bath (reference curve from Figure 1).
(b) The selectivity ratio *$R=J_{Ca}/J_{Na}$* exhibits sharp peaks for the M1 and M2 bands.
(c) *J_{Ca} vs* Ca^{2+} occupancy *P*. The selectivity peaks M1, M2 show saturated conductance at nearly constant *P*.

Mixed salt simulations (Fig. 2 (a)) show that the M1 and M2 J_{Ca} peaks are decreased and shifted to the beginning of the transition regions in P, as compared with the corresponding peaks for a pure Ca^{2+} bath, due to attenuation by Na^+ ions (2). Fig. 2 (b) shows that the selectivity ratio $R=(J_{Ca}/J_{Na})$ peaks at M1 and M2, with $R \approx 150$ for the M1 conduction band, and that there is no selectivity outside these bands. The J vs P plots (Fig. 2 (c)) are each drawn as a J vs $[Ca]$ simulation at constant Q_f. They show that, at $P=1$ for the M1 mode, and $P=2$ for M2, P remains almost constant (saturated) while J increases very rapidly. The saturated conductance appears only for distinct values of Q_f where the output barrier for the bound Ca^{2+} ion falls close to zero due to Coulomb repulsion between the Ca^{2+} ions, leading to barrier-less conduction (14, 19). The arriving ion instantly pushes out and replaces the bound ion, so that P remains constant (14).

The saturated conductance provides the highly selective self-sustained Ca^{2+} flux in a mixed salt bath with a permanently Ca^{2+}-occupied channel that is blocked for Na^+ ions (2).

Because the ion channels of living cells are designed to conduct particular ions selectively, we expect wild-type calcium channels to correspond to one of the high-selectivity bands M1 or M2. Nonselective channels with intermediate Q_f might correspond to mutants. We now argue that, based on their Q_f values and AMFE properties, the M1 and M2 bands correspond respectively to the L-type and RyR calcium channels.
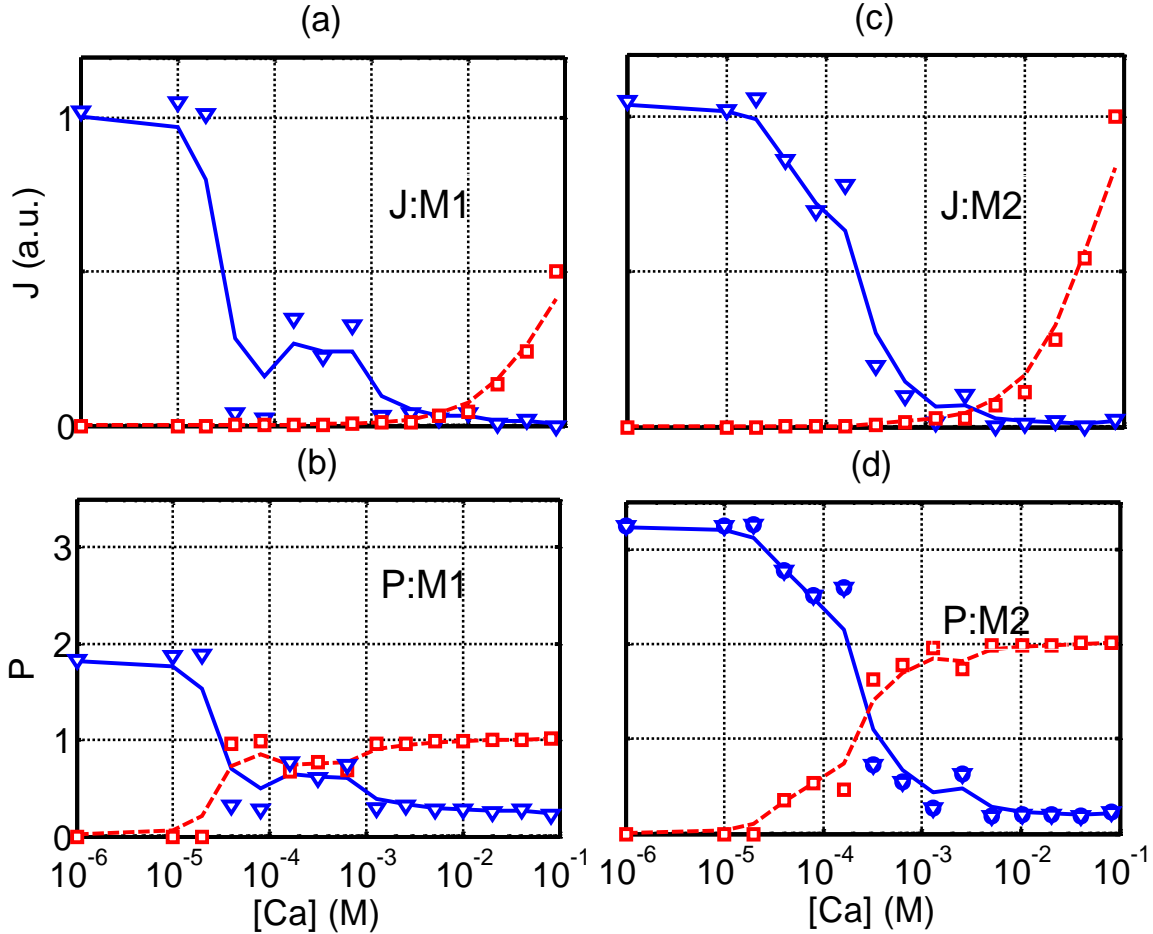

FIGURE 4. AMFE for a mixed salt bath. Sodium (*blue, triangles*) and calcium (*red, squares*) currents *J* and occupancies *P vs* Ca^{2+} concentration *[Ca]* in highly-selective M1 and M2 channels for *[Na]*=30mM.
(a),(b) M1 shows strong blockade and AMFE at P_{Ca}=1 with threshold [Ca]$_{50}$≈ 30μM.
(c),(d) M2 shows blockade and AMFE at P_{Ca}=2, *[Ca]$_{50}$*≈ 0.2mM.

Fig. 3 presents the dependences of *J* and *P* on *[Ca]* for the M1 and M2 bands in a mixed salt configuration. As shown in (a), (b), the M1 band with Q_f=3e shows a strong blockade of the current J_{Na} of Na$^+$ ions with a blockade onset at *[Ca]$_{50}$*≈ 30μM. The blockade occurs after the first Ca^{2+} ion has occupied the SF: P_{Ca}→1. The strong blockade with relatively low onset agrees qualitatively with the observed properties of the L-type channel (1). The value of Q_f, and conduction mechanism for M1 also correspond to the model (2) of the L-type channel.

For the M2 band with $Q_f=5e$ (Fig. 2, (c), (d)) blockade onset occurs at $[Ca]_{50} \approx 0.2$mM, corresponding to double-occupancy of the SF. M2 also shows a larger calcium current than M1. These parameters of AMFE and the value of Q_f can be matched to the RyR channel (4).

The effective parameter values in our model (R, L) can be varied within restricted ranges to fit experimental data for real channels (2, 3). Our parametric study (see Appendix) shows that the simulated bands are only weakly sensitive to variations of R and L in the ranges: R=2.5-3.5Å, L=12-20 Å. Further decrease of L, or increase of R, leads to a weakening of the bands and to their eventual disappearance (at L=8Å for R=3Å). Their disappearance for shorter SFs may be related to the existence of a minimum L needed to hold two Ca^{2+} ions in the SF against their mutual Coulomb repulsion.

Conclusions

In conclusion, self-consistent BD simulations in a reduced model of a calcium channel SF have revealed distinct calcium-selective conduction bands M1 and M2 as a function of Q_f related to integer values of P. The M1 band appears at Q_f=3e with P=1, and the M2 band at Q_f=5e with P=2. The M1 and M2 bands show high calcium selectivity ($R=J_{Ca}/J_{Na}\approx150$ for the M1 band) and prominent AMFE, and can be identified with the L-type and RyR calcium channels, respectively.

Finally, we speculate that gating, and drug-induced blockade, may correspond to switching between a conduction band and a stop-band (18).

Acknowledgements

Appendix: Parametric study

We have performed a parametric study of the stability and variability of the simulated band structure (see main paper) to changes of the effective model parameters: the length L and radius R of the SF, the length H of the charged ring, and the applied voltage V (see FIGURE A1 -FIGURE A4 below). We show that the simulation results are relatively insensitive to changes in the model parameters. Distinct conductivity bands and selectivity bands exist within a range of parameter values, as we now describe in more detail.
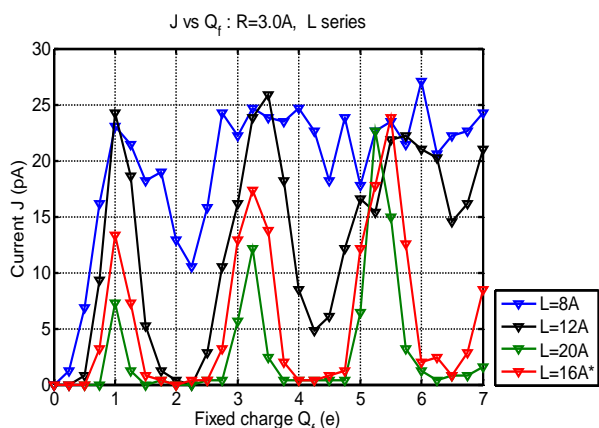

FIGURE A1 Calcium current J vs fixed charge Q_f, showing how the band structure changes as the length of the SF varies in the range L=8-20 Å. Increase of L leads to an increase of the contrast between conduction/non-conduction bands, combined with a decrease of J, and vice versa.
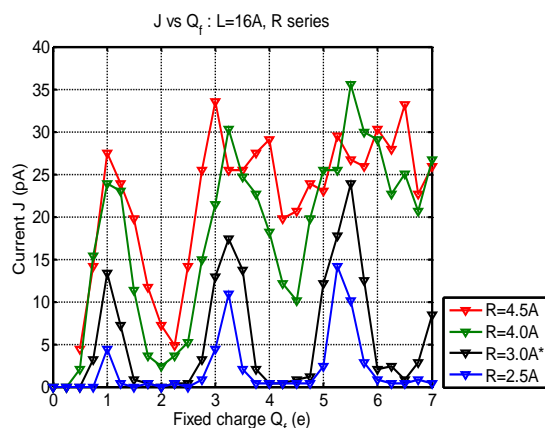
FIGURE A2 Calcium current J vs fixed charge Q_f showing how the band structure changes with the radius of the SF in the range R=2.5-4.5Å. An increase of R to 3-4Å leads to a decrease in the bands' contrast combined with an increase in conductance, but the general pattern of the bands is still visible. A further increase of R to 4.5Å destroys the band structure. A decrease of R to 2.5Å increases the bands' contrast and selectivity but decreases the ion current.

The value of length L for the SF of calcium channels is usually estimated and modelled as being in the range L=5-15Å (2, 3) but the effective length could also depend from the geometry of SF vestibules. We have performed BD simulations with L varying from 8-20 Å to investigate the parametric dependence of the conductance bands on L, as shown in FIGURE A1. An increase in L leads to a sharpening of the band structure and to decreasing conductance. A decrease in L leads to a flattening and eventual disappearance of the band structure (at $L<=10$Å for R=3Å) combined with an increase of conductance.
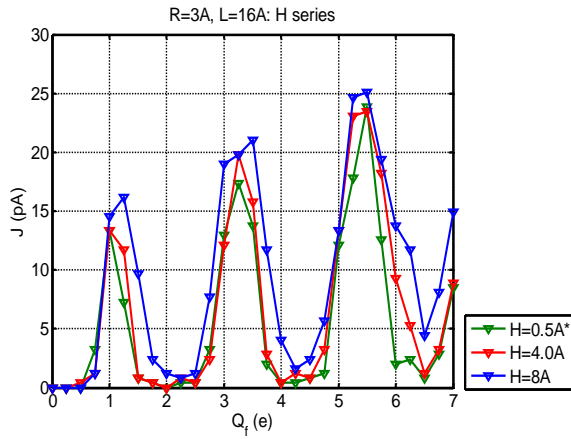
FIGURE A3 Calcium current *J* vs fixed charge *Q*$_f$ showing how the band structure varies with the length of the charged cylindrical ring in the range *H*=0.5-8Å. The band structure is clearly not very sensitive to *H*.
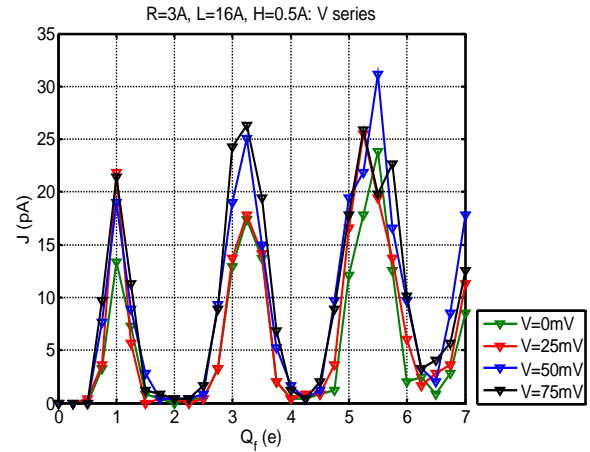
FIGURE A4 Calcium current *J* vs fixed charge *Q*$_f$ showing how the band structure depends on the membrane voltage *V*=0-75mV. It is evident that there is no significant variation with *V*.

We have performed parametric studies to see the effect of varying *R*. FIGURE A2 shows a significant decrease of selectivity with increasing *R*, and vice-versa. The band structure eventually disappears at *R*=4.5A.

We have performed a parametric study using varying lengths *H*=0-8Å of the charged ring. FIGURE A3 shows that the band structure is relatively insensitive to *H*. This finding agrees with the results of dynamic Monte-Carlo simulations (3, 9) for a flexible SF model, which showed that the selectivity is defined by the net charge rather than by a axial distribution of fixed charges.

We have performed a parametric study using varying applied voltage *V*=0-75mV. FIGURE A4 shows that the band structure is relatively insensitive to *V*.

References

1. Sather, W. A., and E. W. McCleskey. 2003. Permeation and Selectivity in Calcium Channels. *Annu. Rev. Physiol.* 65:133-169.

2. Corry, B., T. W. Allen, S. Kuyucak, and S.-H. Chung. 2001. Mechanisms of Permeation and Selectivity in Calcium Channels. *Biophys. J.* 80:195-214.

3. Giri, J., J. Fonseca, D. Boda, D. Henderson, and B. Eisenberg. 2011. Self-organized models of selectivity in calcium channels. *Physical Biology.* 8.

4. Gillespie, D., J. Giri, and M. Fill. 2009. Reinterpreting the Anomalous Mole Fraction Effect: The Ryanodine Receptor Case Study. *Biophys. J.* 97:2212-2221.

5. Burgess, D. L., and J. L. Noebels. 1999. Voltage-Dependent Calcium Channel Mutations in Neurological Disease. *Annals of the New York Academy of Sciences.* 868:199-212.

6. Heinemann, S. H., H. Terlau, W. Stuhmer, K. Imoto, and S. Numa. 1992. Calcium channel characteristics conferred on the sodium channel by single mutations. *Nature.* 356:441-443.

7. Miedema, H., A. Meter-Arkema, J. Wierenga, J. Tang, B. Eisenberg, W. Nonner, H. Hektor, D. Gillespie, and W. Meijberg. 2004. Permeation Properties of an Engineered Bacterial OmpF Porin Containing the EEEE-Locus of Ca2+ Channels. *Biophys. J.* 87:3137-3147.

8. Boda, D., W. Nonner, D. Henderson, B. Eisenberg, and D. Gillespie. 2008. Volume exclusion in calcium selective channels. *Biophys. J.* 94:3486-3496.

9. Csanyi, E., D. Boda, D. Gillespie, and T. Kristof. 2012. Current and selectivity in a model sodium channel under physiological conditions: Dynamic Monte Carlo simulations. *BBA - Biomembranes.* 1818:592-600.

10. Corry, B., T. Vora, and S.-H. Chung. 2005. Electrostatic basis of valence selectivity in cationic channels. *BBA-Biomembranes.* 1711:72-86.

11. Andersen, O. S. 2011. Perspectives on: Ion selectivity. *J. Gen. Physiol.* 137:393-395.

12. Berneche, S., and B. Roux. 2001. Energetics of ion conduction through the K+ channel. *Nature.* 414:73-77.

13. Nelson, P. H. 2011. A permeation theory for single-file ion channels: One- and two-step models. *Biophys. J.* 134:165102.

14. Yesylevskyy, S. O., and V. N. Kharkyanen. 2005. Barrier-less knock-on conduction in ion channels: peculiarity or general mechanism? *Chemical Physics.* 312:127-133.

15. Corry, B., T. Allen, S. Kuyucak, and S. Chung. 2001. Mechanisms of permeation and selectivity in calcium channels. *Biophys. J.* 80:195-214.

16. Hess, P., and R. W. Tsien. 1984. Mechanism of ion permeation through calcium channels. *Nature.* 309:453-456.

17. Hille, B., and W. Schwarz. 1978. Potassium Channels as Multi-Ion Single-file Pores. *J. Gen. Physiol.* 72:409-442.

18. Eisenberg, R. S. 1996. Atomic Biology, Electrostatics and Ionic Channels. In New Developments and Theoretical Studies of Proteins. R. Elber, editor. World Scientific, Philadelphia. 269-357.

19. Kharkyanen, V. N., and S. O. Yesylevskyy. 2009. Theory of single-file multiparticle diffusion in narrow pores. *Phys. Rev. E.* 80:031118.

20. Nadler, B., U. Hollerbach, and R. S. Eisenberg. 2003. Dielectric boundary force and its crucial role in gramicidin. *Phys. Rev. E.* 68:021905.

21. Zhang, J., A. Kamenev, and B. I. Shklovskii. 2005. Conductance of Ion Channels and Nanopores with Charged Walls: A Toy Model. *Phys. Rev. Lett.* 95:148101.

22. Laio, A., and V. Torre. 1999. Physical Origin of Selectivity in Ionic Channels of Biological Membranes. *Biophys. J.* 76:129-148.

23. Tieleman, D. P., P. C. Biggin, G. R. Smith, and M. S. P. Sansom. 2001. Simulation approaches to ion channel structure–function relationships. *QRB.* 34:473-561.

24. Nelissen, K., V. R. Misko, and F. M. Peeters. 2007. Single-file diffusion of interacting particles in a one-dimensional channel. *EPL (Europhysics Letters).* 80:56004.

25. Kittel, C. 2005. Introduction to Solid State Physics. 8th edn. Wiley, New York.